Nonlinear operation of the *Y*-branch switch: Ballistic switching mode at room temperature

Katharina Hieke* and Mikael Ulfward†
Royal Institute of Technology, Electrum 229, S-164 40 Kista-Stockholm, Sweden
(Received 21 June 2000)

We have studied symmetric *Y*-branch switch devices based on InP/InGaAs heterostructures under influence of finite bias between the branches. In this nonlinear operating regime, the applied bias breakes the original geometrical symmetry of the device and a very efficient switching and rectifying properties are observed. These effects are due to ballistic electron propagation, in contrast to conventional rectifying devices relying on depletion in *p-n* junctions. As the ballistic propagation characteristics remain as long as the carrier mean-free-path is not shorter than the device size, we can observe the switching and rectifying behavior even at room temperature.

I. INTRODUCTION

In semiconductor structures with characteristic dimensions smaller than the mean-free-path, electron propagation is ballistic, leading to a variety of nonclassical effects. The *Y*-branch switch (YBS) has been proposed with the aim to realize low (not thermally limited) switching voltages in a single-mode, coherent regime of operation.[1] In this device, electrons are switched from a source to either of two drains (routed) by a lateral electric field, created by gates in the branching region. It has been studied experimentally[2] and theoretically[3] and recently clear indication of coherent transport was found.[4,5]

However, the nonlinear operating regime is of growing interest. For cascaded devices, source-drain voltages in the same order of magnitude as the gate voltages are required. Thus, the *sd* voltages are likely to influence the switching state of the device in a manner similar to the gate voltages, i.e., to cause nonlinearities. In a recent paper,[6] self-gating has been predicted for symmetric single-mode devices. A negative voltage at the reservoir to one branch is transferred into a high electrochemical potential within that branch, and is expected to ''switch off'' this branch, as a negative gate voltage on that side would do. According to this prediction, in an experiment with floating stem, we should always measure a voltage near to the more positive of the two drain voltages. This is in contrast to what we would expect in a classic case or even in the linear coherent regime, where the device symmetry is not changed by the drain voltages and the potential at the stem should be the average of the drain potentials.

In this paper, we present experimental results on YBS devices. A very strong nonlinear behavior was found, making the device similar to a rectifier without classical analog. The results are contrary to the self-gating picture and will be explained by ballistic electron propagation rather than space charge and gating effects.

II. EXPERIMENTAL DETAILS

We have prepared the devices by deep dry etching through a InP/InGaAs based two-dimensional electron gas.

The growth was done by metalorganic vapor phase epitaxy at 650°C on a InP:Fe substrate with the following sequence: 200 nm not intentionally doped (NID) InP, 120 nm InP:Zn (1×10^{17} cm^{-3}), 600 nm NID InP, 10 nm InP:Si (1×10^{18} cm^{-3}), 15 nm NID InP spacer, 12 nm $In_{0.53}Ga_{0.47}As$ quantum well, 15 nm NID InP spacer, 10 nm InP:Si (1×10^{18} cm^{-3}), and 60 nm NID InP top layer. The carrier density N_{2d} and mobility μ in the active layer was determined in standard Hall measurements in a macroscopic Hall bar samples. We found $N_{2d}=1.65(1.3)\times10^{12}$ cm^{-2} and $\mu=1.05\times10^{4}(1.2\times10^{5})$ cm^2/V s at 300 K and 20 K, respectively.

To fabricate nanostructures, patterns were defined on 170 nm thick 950 K PMMA resist by electron-beam lithography with 50 kV accelerating voltage. The mask was then transferred to a 40 nm thick SiN layer by CF_4 reactive ion etching. The semiconductor was deeply etched (through the active layer) by chemically assisted ion-beam etching with acceleration voltage 75 V with Ar. Ohmic contacts were deposited on the capping InP layer and annealed at 425°C. In Fig. 1 a scanning electron microscopy (SEM) micrograph of an YBS device is shown together with a schematic view of the measurement configuration.

The experiments presented in this paper have been carried

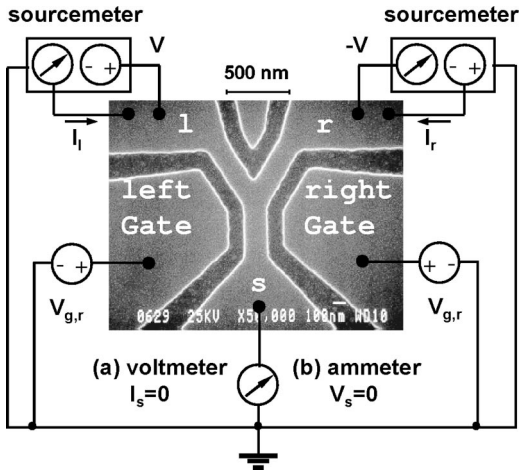

FIG. 1. SEM image of an YBS consisting of 200 nm wide electron waveguides together with a schematic view of the measurement configuration.

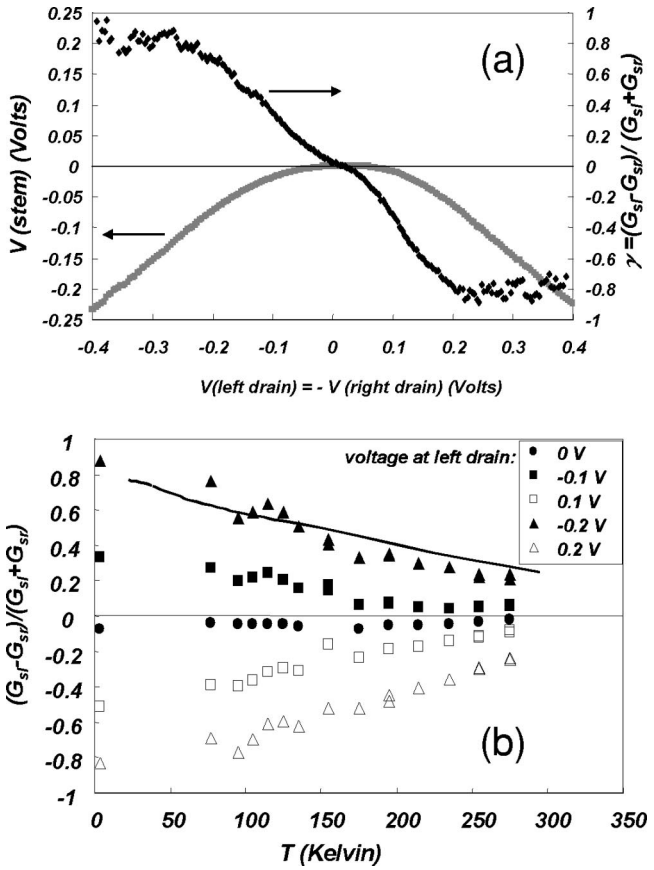

FIG. 2. (a) stem voltage V_s and its derivative $dV_s/dV=\gamma$ versus left branch voltage in a symmetrically biased 200 nm wide YBS with opening angle 30° at $T=77$ K; (b) dependence of γ on temperature for the same device and measurement configuration for different bias; the solid line represents an estimation for the dependence $\gamma(T)$ based on the mean-free-path.

out in dc mode, using Keithley 2400 source meters. The variabel voltages V and $-V$ are applied in a symmetric push-pull manner at the left and right branch (l,r), respectively. We measure in two configurations: (a) the stem voltage V_s is measured as function of V with a high-impedance voltmeter (ensuring that no current flows in the stem) and (b) the stem potential is held at 0 V and the stem current I_s is measured. In both cases, the currents in the left and right branches are measured simultaneously. The influence of the Ohmic contact resistances has been eliminated by separating current and voltage probes at each terminal. The side gates in our structures have been used to apply a bias over the YBS in order to compare the ''external'' and ''internal'' switching efficiency.

III. MEASUREMENT RESULTS AND ANALYSIS

In Fig. 2, V_s is plotted versus V. In this measurement, both side gates were grounded. The measured voltage at the stem is always negative and approximates linear dependence on V for larger bias, with $|dV_s/dV|\approx 0.85$. Note that V is scanned between -0.4 $V\ldots 0.4$ V, which is two orders of magnitude larger than the subband spacing. We have found similar results in a variety of devices, and the effect is largest for small devices and low temperatures.

In order to analyze the experiments systematically, we describe the device as a threeport by means of a conductance matrix $\hat{G}$:

$$d\begin{pmatrix} I_s \\ I_l \\ I_r \end{pmatrix} = \hat{G}\, d\begin{pmatrix} V_s \\ V_l \\ V_r \end{pmatrix} \tag{1}$$

with subscripts s,l,r corresponding to stem, left, and right branches, respectively. Incoming currents in all terminals are counted positive. This generalized voltage-dependent conductance matrix can be defined to relate differential voltages and currents in the YBS. For small bias, this description coincides with the usual expression (for linear response) $\vec{I}=\hat{G}\vec{V}$. Using Kirchhoff's law and the fact that the conductance matrix is symmetric (without external magnetic field), we can write down the general expression:

$$\hat{G}=\begin{pmatrix} -G_{sl}-G_{sr} & G_{sl} & G_{sr} \\ G_{sl} & -G_{sl}-G_{lr} & G_{lr} \\ G_{sr} & G_{lr} & -G_{sr}-G_{lr} \end{pmatrix}. \tag{2}$$

In a geometrically symmetric device without any electromagnetic fields, $G_{sl}=G_{sr}$. We can define the switching parameter $\gamma=(G_{sl}-G_{sr})/(G_{sl}+G_{sr})$; $\gamma=1(-1)$ corresponds to the left branch open (closed) and the right branch closed (open), respectively.

For our two measurement configurations we find (a) for $I_s=0$ and $\vec{V}=(V_s,V,-V)$: $dV_s/dV=\gamma$ and (b) for $\vec{V}=(0,V,-V)$: $dI_s/dV=G_{sr}-G_{sl}$.

The curves in Fig. 2(a) can thus be interpreted in terms of a bias-dependent switching parameter γ. The geometrical symmetry of the devices is broken by the applied bias and the latter is dominating completely. For negative potential at left (right) branch, G_{sl} (G_{sr}) increases and G_{sr} (G_{sl}) decreases. We will refer to this effect as ''ballistic switching mode.'' This very pronounced switching effect is typical for all studied samples and remains partly even at elevated temperature, as will be shown later.

We describe this switching behavior to a ballistic effect within the YBS. Intuitively, it can be understood that an electron which is injected into one branch, will preferentially enter the stem if it is not deflected by an electromagnetic field into the other branch; thus the conductance matrix element for the injection port will increase.

We have changed the measurement configuration to check this explanation qualitatively, see Fig. 3. If the symmetric bias $(V,-V)$ is applied between one branch and the stem, and the resulting potential is measured on the other branch, then the ballistic switching has an asymmetric characteristic and is more effective when the stem is negative. In other words, the more straight the path between electron injection terminal and voltage probe terminal is, the better the coupling is revealed.

A more quantitative theory is based on the model of a YBS as a ballistic cavity, adiabatically coupled via three quantum point contacts (QPC) to the reservoirs, and has been published recently.[7] This theory agrees very well with the

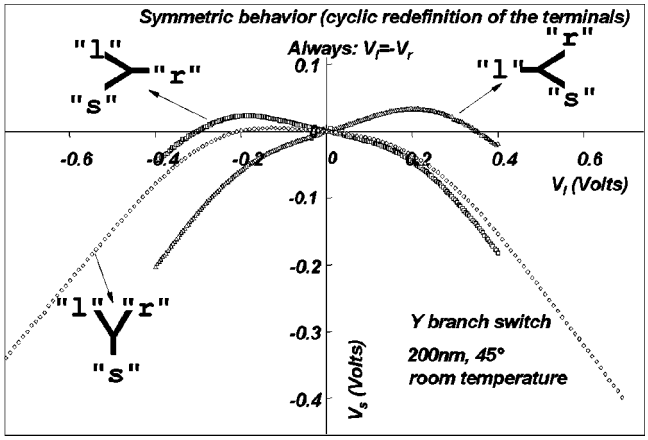

FIG. 3. Measurement of the ballistic switching effect in floating-stem configuration in the same device as 1 at room temperature (curve in the middle) and the same measurement, but with a changed symmetry axis in the devices (the terminals have been ''renamed'') (the outer curves).

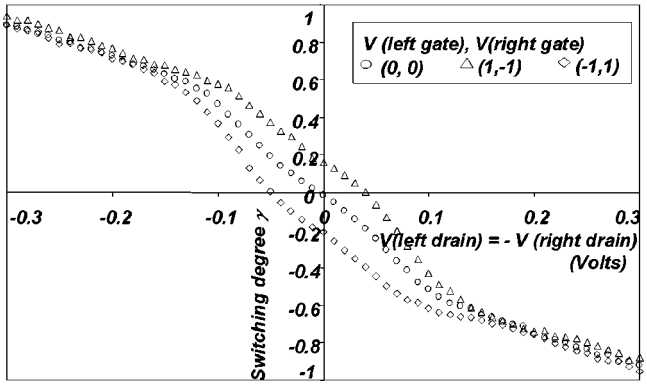

FIG. 4. Comparison of the switching degree vs left branch voltage for the ballistic switching mode and switching by biased side gates. The switching degree γ is plotted for a gate bias of zero, 2 and -2 V for a YBS with 200 nm (opening angle 60°) in a floating-stem configuration at 77 K. The branches are symmetrically biased.

experiments within its whole validity region (bias comparable to the Fermi potential in the device). The theory will be extented to cover the higher biases used in the experiments.

In short, in this article[7] the stem current I_s in a symmetrically biased YBS is calculated in the expression

$$I_s=\frac{2e}{h}\left[\int [N_s(E)-R_{ss}(E)]f(E-\mu_s,T)dE - \sum_{i=l,r}\int T_{si}(E)f(E-\mu_i,T)dE\right], \tag{3}$$

where N_s is the number of occupied $1d$ subbands in the stem, $\mu_{l/r}=\mu_F\pm eV$ the electrochemical potentials in left and right reservoir, and $f(E,T)$ the Fermi-Dirac function. By requiring $I_s=0$, a condition to determine the electrochemical potential in the stem can be found. The transmission probabilities $T_{sl/r}$ between stem and left/right branch and the reflection probability R_{ss} in the stem can be calculated under the assumption that the properties of the YBS are determined by the conductances of the QPCs. Under these conditions, one gets for the stem voltage a quadratic dependence on the bias:

$$V_s=-\frac{1}{2}\alpha V^2, \tag{4}$$

where α is a positive constant, determined by the properties of the QPCs and the temperature.

In Fig. 2(b), γ is shown as a function of the temperature for different bias. At bias 0 V, γ is near 0, independent of the temperature. This is the linear regime in YBS operation and the very small deviation from zero shows that our device is geometrically symmetric in good approximation. When applying finite bias, the device switches into an asymmetric state and the switching degree reduces with increasing temperature. The switching can be made more pronounced even at room temperature by using higher bias. In wider components, however, there is only a very weak asymmetry induced by the bias. For 520 nm wide components, no significant deviation from the symmetric state could be observed at room temperature.

The reduction of the ballistic switching efficiency with increasing temperature and device size is correlated to the mean-free-path L. From Hall measurements, we found that L varies between 2300 nm (at 20 K) and 220 nm (at room temperature). By using the arguments in a recent article,[8] we can estimate that the measured voltage at temperature T is reduced roughly by a factor $(1/2)^{2l/L(T)}$ due to impurity scattering, where l is the characteristic length of the device. The solid curve in Fig. 2(b) is calculated according to this estimation by using the experimentally found dependence $L(T)$, and a good agreement is found. The possibility of ballistic behavior in small InP based components at room temperature has already earlier been demonstrated by the authors.[9]

This ballistic switching effect can be compared with the side-gate switching mode in order to estimate the switching efficiency. In earlier studies on YBS devices in the linear-response mode, the low predicted switching voltages have not yet been achieved due to screening of the applied bias within the structure.[10] In Fig. 4, the switching degree γ is plotted vs the branch bias for three different gate bias configurations. Obviously, the nonlinear ballistic switching is by far the dominating effect. At bias 0 V, the difference in gating degree is 0.35 when changing the gate voltages from (1 V, -1 V) to (-1 V, 1 V). The same switching can be obtained without the gates by varying the branch bias from (0.03 V, -0.03 V) to (-0.03 V, 0.03 V). Thus, the internal ballistic switching is by a factor of approximately 30 more efficient than the external side-gate switching mode. Thus, the observed ballistic switching effect in connection with the low gating efficiency leads to serious complications, if YBS shall be cascaded[11] and the output of one device shall be used to gate another (requiring that sd voltages are of the same order of magnitude as the gate voltages). Further studies are needed to increase the external gating efficiency and to suggest new circuit architecture adapted to the unique internal ballistic switching. In very recent experiments, it has been found that electrochemically deposited Schottky gates

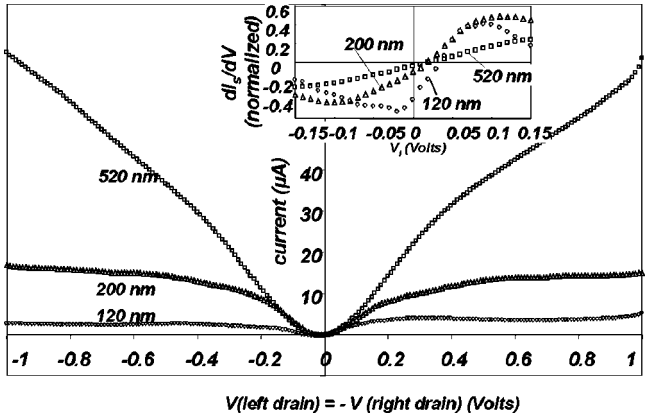

FIG. 5. Comparison of three different YBS with 120 nm, 200 nm, and 520 nm width (opening angle 60°) in a grounded-stem configuration at 77 K. The branches are symmetrically biased. The figure shows the stem current vs left branch bias. In the inset, the normalized derivative dI_s/dV (normalized with the maximum *l*-*r* conductance $dI/2dV(I_s=0,V=0)$ for the respective component) is plotted.

on the sidewalls of the electron waveguide yield about a factor of 10 higher gate efficiency.[5]

The studies of this ballistic switching effect are complemented by measurements in grounded-stem configuration (b). Figure 5 compares the stem current for different components. A finite bias between the branches of the YBS always generates a current in the stem and this stem current has the same sign (namely, electrons are injected from the junction into the stem) independent of the direction of the bias. This result is interpreted as a ballistic rectifying effect, closely related to the ballistic switching above. The total stem current is larger for wider devices than for smaller ones due to the larger intrinsic conductance of wider waveguides. However, the normalized derivative (shown in the inset) which is a measure for the difference between the matrix elements G_{sl} and G_{sr}, is larger for the smaller devices, showing a more efficient ballistic rectifying in those components.

This remarkable ballistic rectifying property is fundamentally different from conventional rectifying devices relying on *p*-*n* junctions. Our YBS rectifier has similarities to the voltage-rectifying four-terminal device presented recently.[8,12] In contrast to that four-terminal device, our YBS does show the unique ballistic behavior over a largely extented bias and temperature region with high efficiency.

In comparison to the predictions[6] of self-gating in YBS with finite bias, our experiments show strong nonlinearities with opposite sign. In the cited publication, a coherent single-mode YBS was studied, and the breaking of the symmetry by bias is ascribed to changed electrochemical potentials within the waveguides near the branching point, creating an electric field over the branching region. Our experimental results can, instead, be explained by the model of a ballistic three-probe cavity.[7] According to that theory, the bias only modifies the conductance of the waveguides but not the properties of the branching region itself, resulting in a quadratical dependence $V_s(|V|)$ (in floating-stem configuration).

Both models are fundamentally different but do not exclude each other. The experiments are likely to show a superposition of both effects, with the ballistic switching by far dominating in our actual configurations. In this context it has to be mentioned that our experiments showed the largest deviations from the mentioned quadratical characteristics at small bias and the lowest temperature. One possible explanation is that both nonlinear effects partially compensate each other in this regime.

To conclude, we have studied YBS devices with a finite bias between the branches. This bias breakes the geometric symmetry of the devices and—depending on the measurement configuration—an efficient switching or rectifying effect can be observed. Those are due to ballistic electron propagation in the devices. Both effects persist partly even at room temperature. The efficiency of the ballistic switching and rectifying is closely related to the ratio between mean-free-path and device size (channel width), explaining both the dependence on temperature and device size.

ACKNOWLEDGMENTS

The authors would like to thank Hongqi Xu, Lukas Worschech, Lars Thylén, and Erik Forsberg for helpful and stimulating discussions and exchange of data and theories prior to publication. Björn Stålnacke and Björn Stoltz helped with the sample fabrication. The authors gratefully acknowledge financial support by the EU LTR research project QSWITCH.

*Email address: hieke@ele.kth.se
†Present affiliation: Ericsson Microelectronics, Kista, Sweden.

[1] T. Palm and L. Thylén, Appl. Phys. Lett. **60**, 237 (1992).
[2] J.-O. J. Wesström, K. Hieke, B. Stålnacke, T. Palm, B. Stoltz, *Proceeding of the 4th International Symposium ECS on Quantum Confinement*, edited by M. Cahay, J. P. Leburton, D. J. Lockwood, and S. Bandyopadhyay (New Jersey, 1997) pp. 221–230.
[3] T. Palm, Phys. Rev. B **52**, 13 773 (1995).
[4] L. Worschech, H. Q. Xu, A. Forchel, and L. Samuelsson (unpublished); private communication.
[5] E. Forsberg and H. Okada (unpublished).
[6] J.-O.J. Wesström, Phys. Rev. Lett. **82**, 2564 (1999).
[7] H. Q. Xu, Phys. Rev. Lett. (to be published).
[8] A.M. Song, Phys. Rev. B **59**, 9806 (1999).
[9] K. Hieke, J.-O.J. Wesström, E. Forsberg, and C.F. Carlström, Semicond. Sci. Technol. **15**, 272 (2000).
[10] K. Hieke, J.-O.J. Wesström, T. Palm, B. Stålnacke, and B. Stoltz, Solid-State Electron. **42**, 1115 (1998).
[11] T. Palm and L. Thylén, J. Appl. Phys. **79**, 8076 (1996).
[12] A.M. Song, A. Lorke, A. Kriele, J.P. Kotthaus, W. Wegscheider, and M. Bichler, Phys. Rev. Lett. **80**, 3831 (1998).